iTRAQ-based Comparative Proteomic Analysis of Flag Leaves of Two Wheat (Triticum aestivum L.) Genotypes Differing in Waterlogging Tolerance at Anthesis

Mingmei Wei
Yangtzeu University
LiuLong Li
Yangtze University
Ke Xie
Beijin University of Science and Technology
Rui Yang
Yangtze University
Xiaoyan Wang
Yangtze University
Aihua Sha (aihuasha@yangtzeu.edu.cn)
Yangtze University

Research article

Keywords: Wheat; Waterlogging; Proteomic; SPAD; qRT-PCR

Posted Date: May 24th, 2019

DOI: https://doi.org/10.21203/rs.2.9778/v1

Abstract

Background Waterlogging is one of the major abiotic stresses limiting wheat product. Plants can adapt to waterlogging with changes in morphology, anatomy, and metabolism. A number of genes or proteins were responsive to waterlogging. Results in this sduty, the iTRAQ-based proteomic strategy was applied to identify waterlogging-responsive proteins in wheat. A total of 7710 proteins were identified in waterlogging tolerant and sensitive wheat varieties XM55 and YM158 at anthesis under waterlogging or not. Sixteen proteins were differentially accumulated between XM55 and YM158 under waterlogging with cultivar specificity. Among them, eleven proteins were up-regulated and five proteins were down-regulated. The up-regulated proteins included Fe-S cluster assembly factor, heat shock cognate 70, GTP-binding protein SAR1A-like, and CBS domain-containing protein. The down-regulated proteins contained photosystem II reaction center protein H, carotenoid 9,10 (9',10')-cleavage dioxygenase-like, psbP-like protein 1, and mitochondrial ATPase inhibitor. In addition, nine proteins were responsive to waterlogging with non-cultivar specificity. These proteins included 3-isopropylmalate dehydratase large subunit, solanesyl-diphosphate synthase 2, DEAD-box ATP-dependent RNA helicase 3, and three predicted or uncharacterized proteins. Sixteen out of the twenty-eight selected proteins showed consistent expression patterns between mRNA and protein levels by quantitative real-time PCR. Conclusions: Our study indicates the much proteins were differential accumulated between the two contrast waterlogging wheat varieties in response to waterlogging, which provide insight into wheat response to waterlogging stress. The identified differentially accumulated protein might be applied to develop waterlogging tolerant wheat.

Background

Waterlogging (WL) is a major abiotic stress that is caused by high rainfall, irrigation practices and/or poor soil drainage [1, 2]. Anoxic soils and severe hypoxia or anoxia within roots often result from WL [2], which affects several physiological processes such as water absorption, hormone relation, ion uptake and transport, and superoxide dismutase activities [3].

Plants can adapt to WL with changes in morphology, anatomy, and metabolism [4]. Development of a shallow root system and formation of aerenchymatous adventitious roots are the main morphological/anatomical changes [5, 6], and are controlled by plant hormones such as ethylene, auxin, abscisic acid (ABA), cytokinin, jasmonates (JAs), and gibberellin (GA) [4]. In rice, lysigenous aerenchyma and a barrier to radial O_2 loss form in roots to mitigate WL stress by supplying O_2 to the root tip [7].

Great efforts were taken to study the mechanism of WL tolerance at the molecular level. Expression levels of many genes were found to change in response to WL by RNA-seq analysis in cotton [8, 9], rapes [10], maize [11, 12], cucumber [13]. Fifty-two and 146 proteins were differentially expressed in tomato leaves and cucumber adventitious roots in response to WL stress, respectively [14, 15]. A total of 100 proteins were found responsive to WL stress in different tissues of WL-sensitive and WL-tolerant barleys [16]. Overexpression of the Kiwifruit AdPDC1 (Actinidia deliciosa pyruvate decarboxylase 1) enhances WL stress resistance in transgenic Arabidopsis thaliana [17].

Wheat (*Triticum aestivum L.*) is one of the most economically important cereal crops in the world. WL has reduced wheat grain yields by about 20-50% in the UK, North America, and Australia [18]. Some attempts have been made to investigate the molecular mechanism responsive to WL in wheat. Transcripts of phenylalanine ammonia-lyase 6, cinnamoyl-CoA reductase 2, ferulate 5-hydroxylase 2 are involved in lignin biosynthesis, and have been shown to be repressed by WL [19]. Genes regulating metabolism of hormones change under WL, which include *ACS7* and *ACO2* for ethylene biosynthesis, *TDC*, *YUC1*, and *PIN9* for indole acetic acid (IAA) biosynthesis/transport, *LOX8*, *AOS1*, *AOC1*, and *JAR1* for JA metabolism, *GA3ox2* and *GA2ox8* for GA metabolism, *IPT5-2*, *LOG1*, *CKX5*, and *ZOG2* for cytokinin metabolism, *NCED1* and *NCED2* for ABA biosynthesis [4]. Anoxia under WL reduces the abundance of denitrification gene *nirS* in the rhizosphere of wheat [20]. However, understanding of the molecular basis of WL tolerance is still limited in wheat.

WL is becoming a major constraint for wheat production in southeast of China due to excessive rainfall during the growing season, which is especially severe during the critical grain formation periods of anthesis and maturation [18, 21]. Proteomics is a useful analytical approach for investigating crop responses to stress by detecting changes in expression and post-translational modification of proteins [22]. Proteomic techniques have been performed to investigate proteins in response to WL in tomato [14], soybean [23], cucumber [15], barley [16], etc. Proteomic approaches have also been successfully used to perform proteomic profiles in response to flooding, drought, high temperature, salt, metal stresses in wheat [24]. In this study, we use proteomics to identify proteins in response to WL in two wheat varieties with different WL tolerances in order to clarify the underlying molecular mechanisms of the WL response in wheat. This work may serve as a resource for the development of WL tolerant wheat varieties.

Results

Phenotypic and Physiological analysis of two varieties

WL is known to induce chlorosis and early senescence of leaves [25]; thus, we initially detected the chlorophyll concentration in expanded flag leaves of waterlogging tolerant variety XM55 and WL sensitive variety YM158 by measuring SPAD (soil-plant analysis development) at the anthesis stage. The SPAD value for XM55 was higher than that for YM158 during days 0-7, and it was less than or equal to that of YM158 during 7-21 d under WL (Fig. 1A). However, SPAD was higher in XM55 than in YM158 between days 0-21 under normal conditions (CK) (Figure. 1A). SPAD of XM55 under normal conditions decreased below that of WL treated XM55 after 7 d, whereas it was decreased below that of YM158 under CK at 5 d (Fig. 1A). The reductions of SPAD in XM55 from 0 to 7 d, 7 to 14 d, and 14 to 21 d under WL were 2.7%, 4.2%, and 7.8%, whereas they were 4.7%, 6.9%, and 13.4% in YM158, respectively.

Soil WL causes serious hypoxia in plant roots, obstructs root growth and development, decreases root activity, and decreases root water permeability; this affects plant water uptake and transpiration rate, thereby leading to water deficit in plants and alterations in the above-ground distribution of water [25, 26]. We also measured the above-ground water contents in the two varieties. Under WL, the water contents in flag leaves, ears, and stem and sheath were significantly higher in XM55 than in YM158 from 7 to 21 d, whereas this pattern occurred from 14 to 21 d under CK (Figure. 1B, C, D)

Waterlogging at elongation or post-anthesis is known to affect grain yield, as well as accumulation and remobilization of dry matter in wheat [26]. We measured the changes of aboveground dry matter accumulation (DMA), yield, and yield-related traits of the two varieties. WL had different effects on XM55 and YM158. The DMA at anthesis (DMA1) before WL were roughly the same among XM55 and YM158, but under WL, DMA2 values were decreased by 12.5% and 20.5% in XM55 and YM158 relative to the CK control at the mature stage, respectively (Table 1). At the same time, kernels per spike, 1000-kernel weight, grain yield weight, and harvest index were decreased under WL by 3.3, 18.1, 26.2 and 15.9% in XM55, and by 10.8, 36.2, 36.8 and 21.8% in YM158 relative to their CK control values, respectively (Table 1). Clearly, WL had greater effects on YM158 than on XM55, especially the 1000-kernel weight and grain yield weight. All together, these suggest that XM55 is more WL tolerant than YM158

Waterlogging Induced Proteome Change in XM55 and YM158

To further explore the molecular mechanisms that lead to the different responses to WL, iTRAQ-based proteomics strategy was applied to analyze proteome changes in flag leaf of both cultivars. After protein extraction, enzyme digestion, iTRAQ labeling, equal mixing and SCX pre-separation, all samples were subjected to LC-MS/MS in three independent replicates. Based on the criteria described in Materials and Methods, a total of 1,087,846 spectra were

detected, among which, 37,952 could be matched and 55,206 were unique spectra, and 37,985 peptides could be identified with 19,279 being unique peptides, and 7710 proteins were identified (Figure. 2A); the proteins identified in the flag leaf of the XM55 and YM158 plants were supported by unique peptides. Of those proteins, 54.0% (4164) were inferred from more than three unique peptides (Figure. 2B).

Comparison of protein changes in XM55 and YM158 under WL

To identify differential protein accumulation between the two cultivars in response to WL, proteins with more than a 1.2-fold change in abundance ($p < 0.05$) between XM55 and YM158 under WL and CK were selected. Based on this criterion, 23 proteins (14 up-regulated and 9 down-regulated) showed differential accumulation between XM55 and YM158 under WL (XM55-WL/YM158-WL), and 52 proteins (31 up-regulated and 21 down-regulated) were differently accumulated between XM55 and YM158 under CK (XM55-CK/YM158-CK) (Fig. 3). At the same time, seven proteins (TRIAE_CS42_2BL_TGACv1_130584_AA0414140.1, TRIAE_CS42_2BL_TGACv1_131439_AA0427700.2, TRIAE_CS42_4BL_TGACv1_321826_AA1065960.1, TRIAE_CS42_2BL_TGACv1_132610_AA0438610.1, TRIAE_CS42_6BL_TGACv1_503168_AA1627380.1, TRIAE_CS42_6BL_TGACv1_503168_AA1627380.2, TRIAE_CS42_6BL_TGACv1_503168_AA1627380.3) were differentially accumulated in both (XM55-WL/YM158-WL) and (XM55-CK/YM158-CK), which might represent cultivar specific protein accumulation irrespective of WL treatment (Fig. 3, Table 2, Table S1). Of the 16 proteins differently accumulated between XM55 and YM158 specifically under WL, 11 were up-regulated; these included members of Fe-S cluster assembly factor, heat shock cognate 70 kDa protein, GTP-binding protein SAR1A-like, and CBS domain-containing protein, respectively. The five down-regulated proteins included photosystem II reaction center protein H, carotenoid 9,10 (9',10')-cleavage dioxygenase-like, psbP-like protein 1, and mitochondrial ATPase inhibitor, respectively (Table 2).

Fe/S clusters participate in diverse cellular processes in almost all organisms, which include respiration, metabolism, DNA replication and repair, and regulation of gene expression [27, 28]. The gene *sufT*, which is involved in the Fe/S cluster assembly pathway, has been shown necessary for effective symbiosis to enhance iron availability [29]. Heat shock cognate 70 kDa protein is a chaperone which assist the folding of other proteins in vivo, and it was found to have increased expression in sugarcane plant subjected to WL [30]. Sar1 in plants showing GTPase activity, cargo secretion, membrane constriction, etc. [31]. Over expression of CBS domain-containing protein could enhance tolerance to different abiotic stresses in tobacco [32] and *Arabidopsis* [33]. These proteins were up-regulated in XM55 compared to YM158 under WL, indicating that their enhanced accumulation may be responsible for WL tolerance.

Photosystem II (PSII) reaction center protein H and psbP are constituents of PS II, which uses light energy to split water into chemical products [34]. Carotenoid cleavage dioxygenases (CCDs) cleave carotenes and xanthophylls to apocarotenoids, which may mediate strigolactone biosynthesis and are responsive to phosphorus deficiency [35], wounding, heat, and osmotic stress [36]. The ATPases play roles in diverse cellular activities such as vesicle-mediated secretion, membrane fusion, cellular organelle biogenesis, and hypersensitive responses (HR) in plants [37]. These proteins were down-regulated in XM55 compared to YM158 under WL, suggesting that WL tolerance might be associated with reduced energy production, changes of hormone content and cellular activities in plants.

Comparison of protein changes in XM55 and YM158 between WL and CK

We also analyzed the differentially accumulated proteins in XM55 and YM158 between WL and CK. There were 84 different proteins (35 up-regulated and 49 down-regulated) between XM55-WL and XM55-CK, and 59 different proteins (13 up-regulated and 46 down-regulated) between YM158-WL and YM158-CK (Figure. 3, TableS2, TableS3). Most proteins responsive to WL were specific to XM55 or YM158. However, Nine proteins were differentially accumulated in both XM55-WL/XM-CK and YM158-WL/YM158-CK (Fig. 3, TableS2, TableS3), which might be WL responsible proteins with non-cultivar specificity. These protein included 3-isopropylmalate dehydratase large subunit (TRIAE_CS42_6AS_TGACv1_487122_AA1568340.1), solanesyl-diphosphate synthase 2 (TRIAE_CS42_1AL_TGACv1_002534_AA0042890.1, TRIAE_CS42_1BL_TGACv1_030959_AA0104550.1, TRIAE_CS42_1DL_TGACv1_063491_AA0227880.1, TRIAE_CS42_1DL_TGACv1_063491_AA0227880.2), DEAD-box ATP-dependent RNA helicase 3 (TRIAE_CS42_4AL_TGACv1_289784_AA0976760.1), and three predicted or Uncharacterized proteins (TRIAE_CS42_4BL_TGACv1_320837_AA1049910.1, TRIAE_CS42_2AL_TGACv1_094081_AA0292320.2

, and TRIAE_CS42_6AS_TGACv1_485670_AA1549870.1).

3-isopropylmalate dehydratase catalyses the stereo-specific isomerization of 2-isopropylmalate and 3-isopropylmalate in the biosynthesis of leucine. Solanesyl-diphosphate synthase 2 is involved in plastoquinone biosynthesis, which regulates gene expression and enzyme activities as a photosynthetic electron carrier, and plays a central photoprotective role as an antioxidant [38]. DEAD-box ATP-dependent RNA helicase 3 is involved in ribosomal structure and it was shown to be markedly suppressed after salt treatment in cotton [39]. These proteins were responsive to waterlogging without cultivar specificity, indicating that the leucine, reactive oxygen species, and the ribosome may play roles in basic defense to WL.

Functional Categorization, Gene Ontology (GO) and Pathway Enrichment Analysis of the Changed proteins

The functional information of all differentially accumulated proteins in Figure 3 were obtained by searching against the UniProt-GOA database, which were assigned to three categories based on GO annotation, that is, cellular compartment, biological process, and molecular function. The differentially expressed proteins among XM55 and YM158 under WL belonged to eight biological processes, 11 cellular compartments, and two different molecular functions (Figure. 4, TableS4). In terms of biological processes, metabolic process, cellular process and cellular component organization or biogenesis were the three major groups. It was suggested that differential expression of proteins are involved in primary metabolic processes, and these impart differential WL tolerances to XM55 and YM158. Cell, cell part, and membrane-enclosed lumen were the top three cellular compartments, implying that various changes in cell structure had effects on tolerance to WL among different varieties. Binding was the major molecular functional groups, and a small amount of differentially accumulated proteins were involved in catalytic activity, which showed that protein binding affects tolerance to WL.

As for the differentially expressed proteins among XM55 or YM158 under WL and CK, they belonged to 11 or eight biological processes, nine or 11 cellular compartments, and six or three molecular functions (FigureS1, FigureS2, TableS4), respectively. Metabolic process, cellular process, and single-organism process were both the three major biological processes. Cell, cell part, and organelle were both the top three cellular compartments. Catalytic activity and binding were both the two major molecular functional groups. Those results indicated that primary metabolic processes, cell structure, and catalytic activity were generally affected by WL regardless of cultivar tolerance.

To characterize the functional consequences of the differentially expressed proteins associated with WL, their pathway enrichments were assigned based on KEGG orthology terms. Only significantly enriched pathway categories that had a p-value lower than 0.05 were selected. The results indicated that the terpenoid backbone biosynthesis, amino sugar and

nucleotide sugar metabolism, and fructose and mannose metabolism were affected by WL in XM55, whereas terpenoid backbone biosynthesis and fatty acid biosynthesis were affected in YM158. Tuberculosis and RNA degradation were affected by WL both in XM55 and YM158 (TableS5).

Correlation of differentially accumulated protein with mRNA Expression

To detect whether the differential expression of proteins was correlated to their mRNA expressions, mRNA levels of 28 differentially expressed proteins were analyzed by qRT-PCR (TableS6). Among them, 16 exhibited consistent expression patterns between mRNAs and proteins, whereas 12 showed discrepancies between protein accumulation and mRNA expression (Figure 5). The discrepancy between protein accumulation and mRNA expressions might be ascribed to translational and posttranslational regulatory processes or feedback loops between the processes of mRNA translation and protein degradation [40]. These results were consistent with previous studies that transcription patterns do not always directly correlate with protein expression levels [16, 41, 42].

Discussion

Wheat is negatively affected by waterlogging stress [43-44], with anthesis being the most sensitive stage [45], during which, waterlogging usually occurs. In this study, we compared the waterlogging tolerance of two wheat varieties, and indicated that waterlogging affected the chlorophyll content, water content, grain weight and its components, and accumulation of dry matter after anthesis in both varieties at anthesis. However, the degree of waterlogging influence varied between the varieties, that is, XM55 was less sensitive to water stress than YM158 (Figure 1 and Table 1).

The proteomics approach was applied to analyze the effects of waterlogging stress on flag leaf proteome pattern during anthesis in tolerant variety XM55 and intolerant variety YM158. Eleven up-regulated proteins in XM55 were identified in response to WL that were involved in iron acquisition [29], proteins folding assistant [30], cargo secretion [31], abiotic stresses [32, 33], whereas five proteins were down-regulated, which participated in light energy usage [34], strigolactone biosynthesis [36], vesicle-mediated secretion [37]. The different tolerance of waterlogging between XM55 and YM158 might be ascribed to those differentially accumulated proteins.

In addition, nine proteins were identified to be responsive to WL with non-cultivar specificity (Fig. 3, TableS2, TableS3), which were involved in leucine biosynthesis, plastoquinone biosynthesis, and ribosomal structure remodelling. Those protein were induced by WL in both WL tolerant and WL non tolerant variety, indicating they played basic roles in defense WL. GO and Pathway Enrichment analysis indicated that proteins involving in primary metabolic processes, cell structure, protein binding determined the different tolerance to WL between XM55 and YM158 (Figure. 4, TableS4).

qRT-PCR analysis indicated that consistent expression patterns were observed between mRNAs and proteins for most selected proteins, however, a discrepancy were also identified for several proteins between protein accumulation and mRNA expression (Figure 5,TableS6). It is suggested that transcription patterns do not always directly correlate with protein expression levels [16, 41, 42], which might be ascribed to translational and posttranslational regulatory processes or feedback loops between the processes of mRNA translation and protein degradation [40].

Conclusions

Our study indicates the much proteins were differential accumulated between the two contrast waterlogging wheat varieties in response to waterlogging. WL causes a redirection in protein synthesis to reduce the synthesis of chlorophyll

and the content of enzymes related to photorespiration in wheat, and influence the synthesis of metabolic enzymes. In addition, the chlorophyll content was reduced and accumulation of harmful metabolites in leaves were increased. It provide insight into wheat response to waterlogging stress, and the identified differentially accumulated protein might be applied to develop waterlogging tolerant wheat.

Methods

Plant growth conditions and treatments

The wheat cultivars XM55 and YM158 were used in the screen for WL-responsive proteins. They were sown in the farm of Yangtze University located in Jingzhou of Hubei Province, China in growing seasons on November 15, 2017. The topsoil (0-20 cm) of the experimental field is a clay loam and the nutrient status was as follows, organic matter content was 10.5 $g \cdot kg^{-1}$; available N concentration was 33.41 $mg \cdot kg^{-1}$; available P_2O_5 concentration was 45.37 $mg \cdot kg^{-1}$; and available K_2O concentration was 80.26 $mg \cdot kg^{-1}$.

The field experiments were conducted with 2 treatments; The WL treatment consisted of wheat at anthesis treated with WL for 7 days, and wheat at anthesis without WL treatment served as the control. Three replicates were performed per treatment for each variety, and the plot areas were 12 m^2 (2 m × 6 m). At the sowing stage, the base application rate was 90 kg/hectare of pure nitrogen from the application of compound fertilizer, and the ratio of available nitrogen N, phosphorus P_2O_5 and potassium K_2O in compound fertilizer was 26:10:15. At the jointing stage, pure nitrogen was applied at 90 kg/hectare in the form of urea. At the trefoil stage, 224 plants m^{-2} remained. Otherwise, regular field management practices were employed. Wheat plants for both cultivars at anthesis stage were subjected to control and waterlogging treatment for 7 d. The samples were collected, immediately frozen, and stored in liquid nitrogen for protein and RNA extraction for qRT-PCR. Material was collected from ten plants per sample, and three biological replicates were conducted for each treatment.

Protein extraction, digestion and iTRAQ labelling

Total protein was extracted using the cold acetone method. Samples were ground to powder in liquid nitrogen, then dissolved in 2 mL lysis buffer (8 M urea, 2% SDS, 1x Protease Inhibitor Cocktail (Roche Ltd. Basel, Switzerland), followed by sonication on ice for 30 min and centrifugation at 13 000 rpm for 30 min at 4℃. The supernatant was transferred to a fresh tube. For each sample, proteins were precipitated with ice-cold acetone at -20℃ overnight. The precipitate was cleaned with acetone three times and re-dissolved in 8M Urea by sonication on ice. Protein quality was determined by SDS-PAGE.

BCA protein assay (Pierce, MA, USA) was used to determine the protein concentration of the supernatant. 100 μg protein per condition was transferred into a new tube and adjusted to a final volume of 100 μL with 8M Urea. 11 μL of 1M DTT (DL-Dithiothreitol) was added and samples were incubated at 37°C for 1hour. Then 120 μL of the 55 mM iodoacetamide was added to the sample and incubated for 20 minutes at room temperature in the dark.

For each sample, proteins were precipitated with ice-cold acetone, then re-dissolved in 100 μL TEAB. Proteins were then tryptic digested with sequence-grade modified trypsin (Promega, Madison, WI) at 37°C overnight. The resultant peptide mixture was labeled with iTRAQ tags 113 through 118. The labeled samples were combined and dried in vacuum.

Strong cation exchange (SCX) fractionation and liquid chromatography–tandem mass spectrometry (LC-MS/MS) analysis

The combined labeled samples were bound to a SCX fractionation column connected with a high performance liquid chromatography (HPLC) system. The peptide mixture was re-dissolved in the buffer A (20mM ammonium formate in water, pH10.0, adjusted with ammonium hydroxide), and then fractionated by high pH separation using Ultimate 3000 system (Thermo Fisher scientific, MA, USA) connected to a reverse phase column (XBridge C18 column, 4.6 mm x 250 mm, 5 μm, (Waters Corporation, MA, USA). High pH separation was performed using a linear gradient starting from 5% B to 45% B in 40 min (B: 20 mM ammonium formate in 80% ACN, pH 10.0, adjusted with ammonium hydroxide). The column was re-equilibrated at initial conditions for 15 min. The column flow rate was maintained at 1mL/min and column temperature was maintained at 30℃. Twelve fractions were collected; each fraction was dried in a vacuum concentrator for the next step.

Peptide fractions were resuspended with 30 μL solvent C respectively (C: water with 0.1% formic acid; D: ACN with 0.1% formic acid), separated by nanoLC and analyzed by on-line electrospray tandem mass spectrometry. The experiments were performed on an Easy-nLC 1000 system (Thermo Fisher Scientific, MA, USA) connected to a Orbitrap Fusion Tribrid mass spectrometer (Thermo Fisher Scientific, MA, USA) equipped with an online nano-electrospray ion source. 10 μL peptide sample was loaded onto the trap column (Thermo Scientific Acclaim PepMap C18, 100 μm × 2 cm), with a flow of 10 μL/min for 3 min and subsequently separated on the analytical column (Acclaim PepMap C18, 75 μm × 15 cm) with a linear gradient, from 3% D to 32% D in 120 min. The column was re-equilibrated at initial conditions for 10 min. The column flow rate was maintained at 300 nL/min. The electrospray voltage of 2 kV versus the inlet of the mass spectrometer was used.

The fusion mass spectrometer was operated in the data-dependent mode to switch automatically between MS and MS/MS acquisition. Survey full-scan MS spectra (m/z 350-1550) were acquired with a mass resolution of 120 K, followed by sequential high energy collisional dissociation (HCD) MS/MS scans with a resolution of 30 K. The isolation window was set as 1.6 Da. The AGC target was set as 400000. MS/MS fixed first mass was set at 110. In all cases, one microscan was recorded using dynamic exclusion of 45 seconds.

Database search

The mass spectrometry data were transformed into MGF files with Proteome Discovery 1.2 (Thermo, Pittsburgh, PA, USA) and analyzed using Mascot search engine (Matrix Science, London, UK; version 2.3.2). Mascot database was set up for protein identification using *Triticum aestivum L* reference transcriptome or *Triticum aestivum L* database in NCBInr/SwissProt/Uniprot/IPI. Mascot was searched with a fragment ion mass tolerance of 0.050 Da and a parent ion tolerance of 10.0 PPM.

Protein identification and quantification

The Mascot search results were averaged using medians and quantified. Proteins with fold change in a comparison ≥1.2 or ≤0.83 and unadjusted significance level $p < 0.05$ were considered differentially expressed.

GO Enrichment analysis

Gene Ontology (GO) is an international standardized gene functional classification system which offers a dynamic-updated controlled vocabulary and a strictly defined concept to comprehensively describe properties of genes and their products in any organism. GO has three ontologies: molecular function, cellular component and biological process. The basic unit of GO is GO-term. Each GO-term belongs to a type of ontology.

GO enrichment analysis provides all GO terms that were significantly enriched in DEGs comparing to the genome background, and can filter DEGs that correspond to biological functions. Initially, all DEGs were mapped to GO terms in the Gene Ontology database (http://www.geneontology.org/); gene numbers were calculated for every term. The hypergeometric test was used to determine significant enrichment of GO terms in DEGs relative to the genome background. The calculated p-value was put through FDR Correction, taking FDR≤ 0.05 as a threshold. GO terms meeting this condition were defined as significantly enriched GO terms in DEGs. This analysis was able to recognize the main biological functions that DEGs exercise.

Pathway enrichment analysis

Pathway-based analysis was conducted by blasting against for KEGG database [46]. Pathway enrichment analysis identified significantly enriched metabolic or signal transduction pathways with DEGs relative to the whole genome background. The calculated p-value was put through FDR Correction, taking FDR≤ 0.05 as a threshold. Pathways meeting this condition were defined as significantly enriched pathways in DEGs.

RNA extraction and qRT-PCR

Total RNA was extracted using the TRIZOL reagent (Invitrogen, Carlsbad, CA, USA), and then treated with RNase free DNase (Invitrogen, Gaithersburg, MD, USA). The purified RNA was reverse transcribed using the RevertAid^{TM} First Strand cDNA Synthesis Kit (Thermo Fisher Scientific) according to the manufacturer's protocol. The qRT-PCR reactions were performed in CFX96^{TM} Real-Time PCR Detection System (Bio-Rad, USA). Gene specific primers are listed in Table S6. Each reaction was conducted in 10 μL mixture containing 5 μL of SYBR green (SYBR$^{@}$ Premix Ex Taq^{TM} (TliRNaseH Plus), TAKARA, Japan), 0.3 μL forward and reverse primers (10 μM), respectively, 2 μL cDNA template, and 2.4 μL ddH_2O. The reactions for each gene were conducted in triplicate with the thermal cycling conditions as follows: 95 °C for 30 s, followed by 40 cycles of 95 °C for 5 s and 57 °C for 30 s. The primer specificity was confirmed by melting curve analysis. Relative expression levels of the genes were calculated using the $2^{-\Delta\Delta CT}$ method [47].

Abbreviations

qRT-PCR: quantitative real-time PCR ABA: abscisic acid JAs: Jasmonates

AdPDC1: Actinidia deliciosa pyruvate decarboxylase 1 IAA: Indole acetic acid

GA: Gibberellin PSII: Photosystem II HR: Hypersensitive responses

DEGs: different expression genes WL: Waterlogging CK: Normal conditions

DMA: Dry matter accumulation CCDs: Carotenoid cleavage dioxygenases

GO: Gene Ontology SCX: Strong cation exchange

LC-MS/MS: Liquid chromatography–tandem mass spectrometry

Declarations

Acknowledgments

Not applicable.

Funding

This work was supported by the National Key Research and Development Program of China (2016YFD0300107, 2017YFD0300202-3) and the National Natural Science Foundation of China (31371580□31871578).

Availability of data and materials

All data generated or analyzed during this study are included in this published article and its supplementary information files.

Authors' Contributions

XW and AS designed the experiments. MW conducted ITRAQ experiments. LL conducted biologic information analysis. RY conducted qRT-PCR. KX conducted waterlogging phenotype collection. MW, LL, and KX wrote the manuscript.

Ethics approval and consent to participate

Not applicable.

Consent for publication

Not applicable.

Competing interests

The authors declare that they have no competing interests.

References

1. Ahmed F, Rafii M, Ismail M, Juraimi A, Rahim H, Asfaliza R, Latif M. Waterlogging tolerance of crops: breeding, mechanism of tolerance, molecular approaches, and future prospects. Biomed Res Int. 2013; 963525.

2. Herzog M, Striker G, Colmer T, Pedersen O. Mechanisms of waterlogging tolerance in wheat-a review of root and shoot physiology. Plant Cell Environ. 2016; 39(5): 1068-86.

3. Ghobadi ME, Ghobadi M, Zebarjadi A. Effect of waterlogging at different growth stages on some morphological traits of wheat varieties. Int J Biometeorol. 2017; 67.

4. Nguyen T, Tuan P, Mukherjee S, Son S, Ayele B. Hormonal regulation in adventitious roots and during their emergence under waterlogged conditions in wheat. J Exp Bot. 2018; 69(16): 4065-82.

5. Bailey-Serres J, Lee SC, Brinton E. Waterproofing crops: effective flooding survival strategies. Plant Physiol. 2012; 160: 1698-709.

6. Yamauchi T, Colmer TD, Pedersen O, Nakazono M. Regulation of root traits for internal aeration and tolerance to soil waterlogging-flooding stress. Plant Physiol. 2018; 176(2):1118-30.

7. Nishiuchi S, Yamauchi T, Takahashi H, Kotula L, Nakazono M. Mechanisms for coping with submergence and waterlogging in rice. Rice. 2012; 5: 2.

8. Christianson J, Llewellyn D, Dennis E, Wilson I. Global Gene Expression Responses to Waterlogging in Roots and Leaves of Cotton (Gossypium hirsutum L.). Plant Cell Physiol. 2010; 51(1): 21-37.

9. Zhang Y, Kong X, Dai J, Luo Z.; Li Z, Lu H, Xu S, Tang W, Zhang D, Li W, Xin C, Dong H. Global gene expression in cotton (Gossypium hirsutum L.) leaves to waterlogging stress. Plos One. 2017; 12(9): e0185075.

10. Lee YH, Kim KS, Jang YS, Hwang JH, Lee DH, Choi IH. Global gene expression responses to waterlogging in leaves of rape seedlings. Plant Cell Rep. 2014; 33: 289-99.

11. Du HW, Zhu JX, Su H, Huang M, Wang HW, Ding SC, Zhang BL, Luo A, Wei SD, Tian XH, Xu YB. Bulked segregant RNA-seq reveals differential expression and snps of candidate genes associated with waterlogging tolerance in maize. Front Plant Sci. 2017; 8: 1022.

12. Arora K, Panda KK, Mittal S, Mallikarjuna MG, Rao AR, Dash PK, Thirunavukkarasu N. RNAseq revealed the important gene pathways controlling adaptive mechanisms under waterlogged stress in maize. Scientific Reports. 2017; 7: 10950.

13. Qi XH, Xu XW, Lin XJ, Zhang WJ, Chen XH. Identification of differentially expressed genes in cucumber (Cucumis sativus L.) root under waterlogging stress by digital gene expression profile. Genomics. 2012; 99: 160-8.

14. Ahsana N, Lee DG, Lee SH, Kang KY, Bahk JD, Choi MS, Lee IJ, Renaut J, Lee BH. A comparative proteomic analysis of tomato leaves in response to waterlogging stress. Physiol Plant. 2007; 131: 555-0.

15. Xu XW, Ji J, Ma XT, Xu Q, Qi XH, Chen XH. Comparative proteomic analysis provides insight into the key proteins involved in cucumber (Cucumis sativus L.) adventitious root emergence under waterlogging stress. Front Plant Sci. 2016; 7: 1515.

16. Luan HY, Shen HQ, Pan YH, Guo BJ, Lv C, Xu RG. Elucidating the hypoxic stress response in barley (Hordeum vulgare L.) during waterlogging: A proteomics approach. Scientific Reports. 2018; 8: 9655.

17. Zhang JY, Huang SN, Wang G, Xuan JP, Guo ZR. Overexpression of Actinidia deliciosa pyruvate decarboxylase 1 gene enhances waterlogging stress in transgenic Arabidopsis thaliana. Plant Physiology and Biochemistry. 2016; 106: 244e252.

18. Li CY, Jiang D, Wollenweber B, Li Y, Dai TB, Cao WX. Waterlogging pretreatment during vegetative growth improves tolerance to waterlogging after anthesis in wheat. Plant Science. 2011; 180: 672-8.

19. Nguyen TN, Son SH, Jordan MC, Levin DB, Ayele BT. Lignin biosynthesis in wheat (Triticum aestivum L.): its response to waterlogging and association with hormonal levels. BMC Plant Biology. 2016; 16: 28.

20. Hamonts K, Clough TJ, Stewart A, Clinton PW, Richardson AE, Wakelin SA, O'Callaghan M, Condron LM. Effect of nitrogen and waterlogging on denitrifier gene abundance, community structure and activity in the rhizosphere of wheat. FEMS Microbiol Ecolo. 2013; 83: 568-84.

21. Jiang D, Fan XM, Dai TB, Cao WX. Nitrogen fertiliser rate and post-anthesis waterlogging effects on carbohydrate and nitrogen dynamics in wheat. Plant Soil. 2008; 304: 301-14.

22. Komatsu S, Hiraga S, Yanagawa Y. Proteomics Techniques for the Development of Flood Tolerant Crops. J Proteome Res. 2012; 11: 68-78.

23. Alam I, Lee DG, Kim KH, Park CH, Sharmin SA, Lee H, Oh KW, Yun BW, Lee BH. Proteome analysis of soybean root under waterlogging stress at an early vegitatibe stage. J Biosci. 2010; 35: 49-62.

24. Komatsu S, Kamal AHM, Hossain Z. Wheat proteomics: proteome modulation and abiotic stress acclimation. Front Plant Sci. 2014; 5: 684

25. Romina P, Abeledo LG, Miralles DJ. Identifying the critical period for waterlogging on yield and its components in wheat and barley. Plant Soil. 2014; 378: 265-77.

26. Lina J, Shan X, Jiang C, Hongjian G, Ligan Z. The effect of persistent flooding on the kinetic nutrient absorption and output of wheat. J Chinese Agricultural Science Bulletin. 2012; 28(27): 113-7.

27. Beinert H, Holm RH, Münck E. Iron-sulfur clusters: nature's modular, multipurpose structures. Science. 1997; 277: 653-9.

28. Lill R. Function and biogenesis of iron-sulphur proteins. Nature. 2009; 460: 831-8.

29. Sasaki S, Minamisawa K, Mitsui H. A Sinorhizobium meliloti RpoH-Regulated Gene Is Involved in Iron-Sulfur Protein Metabolism and Effective Plant Symbiosis under Intrinsic Iron Limitation. J Bacteriol. 2016; 198: 2297-306.

30. Khan MS, Khraiwesh B, Pugalenthi G, Gupta RS, Singh J, Duttamajumder SK, Kapur R. Subtractive hybridization-mediated analysis of genes and in silico prediction of associated microRNAs under waterlogged conditions in sugarcane (Saccharum spp.). FEBS Open Bio. 2014; 4: 533-41.

31. Zeng Y, Chung K, Li B, Lai C, Lam S, Wang X, Cui Y, Gao C, Luo M, Wong K, Schekman R, Jiang L. Unique COPII component AtSar1a/AtSec23a pair is required for the distinct function of protein ER export in Arabidopsis thaliana. Proc Natl Acad Sci USA. 2015; 112(46): 14360-5.

32. Singh AK, Kumar R, Pareek A, Sopory SK, Singla-Pareek SL. Overexpression of rice CBS domain containing protein improves salinity, oxidative, and heavy metal tolerance in transgenic tobacco. Mol Biotechnol. 2012; 52: 205-16.

33. Hao Q, Shang W, Zhang C, Chen H, Chen L, Yuan S, Chen S, Zhang X, Zhou X. Identification and Comparative Analysis of CBS Domain-Containing Proteins in Soybean (Glycine max) and the Primary Function of GmCBS21 in Enhanced Tolerance to Low Nitrogen Stress. Int J Mol Sci. 2016; 17(5): 620.

34. Vinyard DJ, Ananyev GM, Dismukes GM. Photosystem II: The Reaction Center of Oxygenic Photosynthesis. Annu Rev Biochem. 2013; 82: 577-606

35. Pan XY, Zheng HY, Zhao JY, Xu YJ, Li XX. ZmCCD7/ZpCCD7 encodes a carotenoid cleavage dioxygenase mediating shoot branching. Planta. 2016; 243(6): 1407-18.

36. Rubio-Moraga A, Rambla JL, Fernández-de-Carmen A, Trapero-Mozos A, Ahrazem O, Orzáez D, Granell A, Gómez-Gómez L. New target carotenoids for CCD4 enzymes are revealed with the characterization of a novel stress-induced carotenoid cleavage dioxygenase gene from Crocus sativus. Plant Mol Biol. 2014; 86(4-5): 555-69.

37. Baek K, Seo PJ, Park CM. Activation of a Mitochondrial ATPase Gene Induces abnormal Seed Development in Arabidopsis. Mol Cells. 2011; 31(4): 361-9.

38. Ksas B, Becuwe N, Chevalier A, Havaux M. Plant tolerance to excess light energy and photooxidative damage relies on plastoquinone biosynthesis. Sci Rep. 2015; 5: 10919.

39. Gong W, Xu F, Sun J, Peng Z, He S, Pan Z, Du X. iTRAQ-Based Comparative Proteomic Analysis of Seedling Leaves of Two Upland Cotton Genotypes Differing in Salt Tolerance. Front Plant Sci. 2017; 8: 2113.

40. Ahsan N, Lee DG, Lee SH, Kang KY, Bahk JD, Choi MS, Lee IJ, Renaut J, Lee BH. A comparative proteomic analysis of tomato leaves in response to waterlogging stress. Physiol Plant. 2007; 131: 555-70.

41. Yan SP, Zhang QY, Tang ZC, Su WA, Sun WN. Comparative proteomic analysis provides new insight into chilling stress response in rice. Mol Cell Proteomics. 2006; 5: 484-96.

42. Mano Y, Omori F. Flooding tolerance in interspecific introgression lines containing chromosome segments from teosinte (Zea nicaraguensis) in maize (Zea mays subsp.mays). Annals of Botany. 2013; 112: 1125-39.

43. Ding JF, Su SN, Liang P. Effect of waterlogging at elongation or after anthesis on grain yield and remobilization of dry matter and nitrogen in wheat. Journal of Triticeae Crops. 2017; 37(11): 1473-79.

44. Araki H, Hamada A, Hossain M, Takahashi T. Waterlogging at jointing and/or after anthesis in wheat induces early leaf cence and impairs grain filling. Field Crops Research. 2012; 137: 27-36.

45. Li CY, Cai J, Jiang D, Dai TB, Cao WX. Effects of hardening by pre-anthesis waterlogging on grain yield and quality of post-anthesis waterlogging wheat (Triticum aestivum L. cv Yangmai 9). Acta Ecologica Sinica. 2011; 31: 1904-10.

46. Jia XY, He LH, Jing RL, Li RZ. Calreticulin: conserved protein and diverse functions in plants. Physiol Plant. 2009; 136: 127-38.

47. Kim J, Nguyen N, Nguyen N, Hong S, Lee H. Loss of all three calreticulins, CRT1, CRT2 and CRT3, causes enhanced sensitivity to water stress in Arabidopsis. Plant Cell Rep. 2013; 32: 1843-3.

Tables

Table 1 Effect of waterlogging on yield and yield components of wheat

Cultivar	Treatment	DMA1 (g stem-1)	DMA2 (g stem-1)	Kernel per spike	1000-kernel weight (g)	Grain yield weight (g stem-1)	Harvest index
XM55	CK	2.07a	3.21b	43.31b	29.33b	1.41b	0.44b
	WL	2.1a	2.81c	41.87b	24.02c	1.04c	0.37c
	(WL-CK)/CK	/	0.125	0.033	0.181	0.262	0.159
YM158	CK	2.19a	3.57a	45.47a	34.47a	1.63a	0.46a
	WL	2.17a	2.84c	41.56b	25.31c	1.03c	0.36c
	(WL-CK)/CK	/	0.205	0.108	0.362	0.368	0.218

The lowercase letters indicate significant differences at $P<0.05$ among treatments as determined by Duncan's Multiple Range Test. DMA1, aboveground dry matter accumulation at anthesis before waterlogging；DMA2, aboveground dry matter accumulation at maturity; CK, Control; WL, Waterlogging

Table 2. Differentially expressed proteins between XM55 and YM158 under WL

Gene ID	log2_FC (XM55/YM158)	Protein Description	Functional Category
UP-regulated			
TRIAE_CS42_2BL_TGACv1_130584_AA0414140.1	1.63	Ubiquinol oxidase 4	redox
TRIAE_CS42_2BL_TGACv1_131439_AA0427700.2	1.50	Superoxide dismutase [Mn],	redox
TRIAE_CS42_4BL_TGACv1_321826_AA1065960.1	1.18	heat shock protein 101	stress response
TRIAE_CS42_3AL_TGACv1_195570_AA0651350.1	0.33	Fe-S cluster assembly factor HCF101	chloroplast
TRIAE_CS42_3AL_TGACv1_195570_AA0651350.2	0.33	Fe-S cluster assembly factor HCF101	chloroplast
TRIAE_CS42_3AL_TGACv1_195570_AA0651350.3	0.33	Fe-S cluster assembly factor HCF101	chloroplast
TRIAE_CS42_3DL_TGACv1_250912_AA0874940.1	0.33	Fe-S cluster assembly factor HCF101	chloroplast
TRIAE_CS42_3DL_TGACv1_250912_AA0874940.2	0.33	Fe-S cluster assembly factor HCF101	chloroplast
TRIAE_CS42_2BL_TGACv1_131039_AA0421600.2	0.32	heat shock cognate 70 kDa protein 2-like	transcription
TRIAE_CS42_6DL_TGACv1_526647_AA1688990.1	0.32	heat shock cognate 70 kDa protein 2-like	transcription
TRIAE_CS42_3AS_TGACv1_211332_AA0688720.1	0.31	GTP-binding protein SAR1A-like	GTP binding
TRIAE_CS42_3DS_TGACv1_272355_AA0919480.1	0.31	GTP-binding protein SAR1A-like	GTP binding
TRIAE_CS42_6DL_TGACv1_526455_AA1684150.2	0.29	CBS domain-containing protein	
TRIAE_CS42_6DL_TGACv1_526455_AA1684150.3	0.29	CBS domain-containing protein	
Down-regulated			
AIG90456	-0.26	photosystem II reaction center protein H	plastid
TRIAE_CS42_5DS_TGACv1_456540_AA1473460.1	-0.36	carotenoid 9,10(9',10')-cleavage dioxygenase-like	stress response
TRIAE_CS42_4BS_TGACv1_330468_AA1107820.2	-0.67	psbP-like protein 1, chloroplastic	metabolic
TRIAE_CS42_4BS_TGACv1_329474_AA1101780.1	-0.87	mitochondrial ATPase inhibitor	photorespiration
TRIAE_CS42_4BS_TGACv1_329474_AA1101780.3	-0.87	mitochondrial ATPase inhibitor	photorespiration
TRIAE_CS42_2BL_TGACv1_132610_AA0438610.1	-1.29	Aminomethyltransferase	redox
TRIAE_CS42_6BL_TGACv1_503168_AA1627380.1	-0.78	Uncharacterized protein	

TRIAE_CS42_6BL_TGACv1_503168_AA1627380.2	-0.78	Uncharacterized protein
TRIAE_CS42_6BL_TGACv1_503168_AA1627380.3	-0.78	Uncharacterized protein

Figures

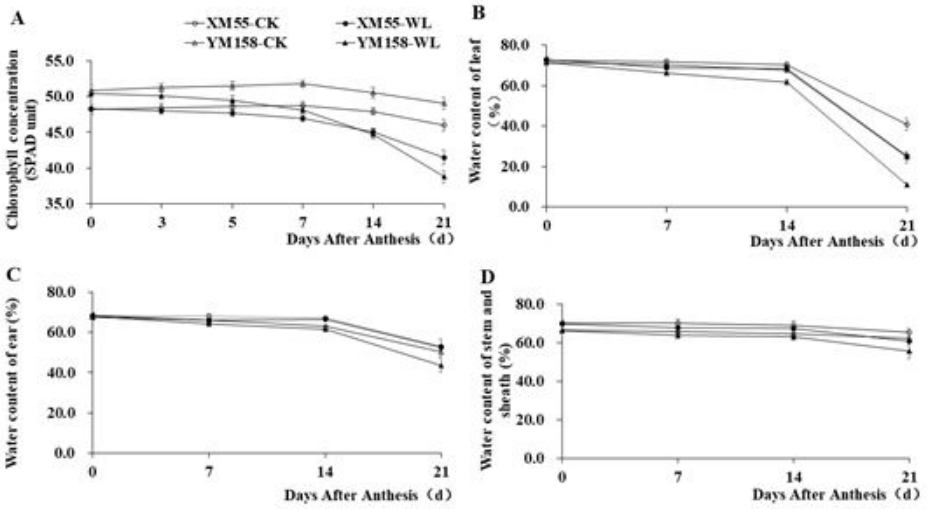

Figure 1

Phenotypes of XM55 and YM158 under waterlogging and control conditions. (A) dynamic changes of chlorophyll concentration (SPAD unit) of the last expanded leaf after 7 days waterlogging at anthesis; (B) dynamic changes of water content of leaf after waterlogging at anthesis between different varieties; (C) dynamic changes of ear water content after waterlogging at anthesis between different varieties; (D) dynamic changes of water content of stem and sheath after waterlogging at anthesis between different varieties.

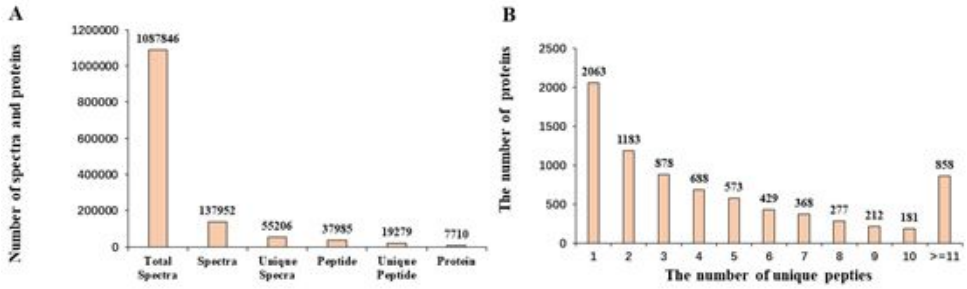

Figure 2

Mass spectrometry analysis and protein identification. A, the number of spectra and proteins. B, the number of proteins with different unique peptides.

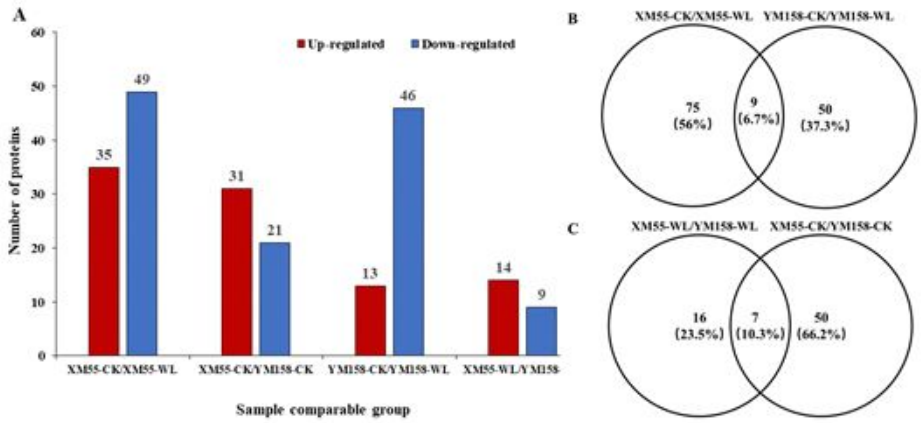

Figure 3

Quantitative and Venn analysis of the proteome of two wheat cultivars under different treatments. (A) Quantitative analysis of the proteome between the waterlogging treated and control samples; (B) Venn analysis of two wheat cultivars under different treatments; (C) Venn analysis of different treatments in different wheat cultivars; XM55 and YM158 are the two cultivars; CK, control; WL, waterlogging

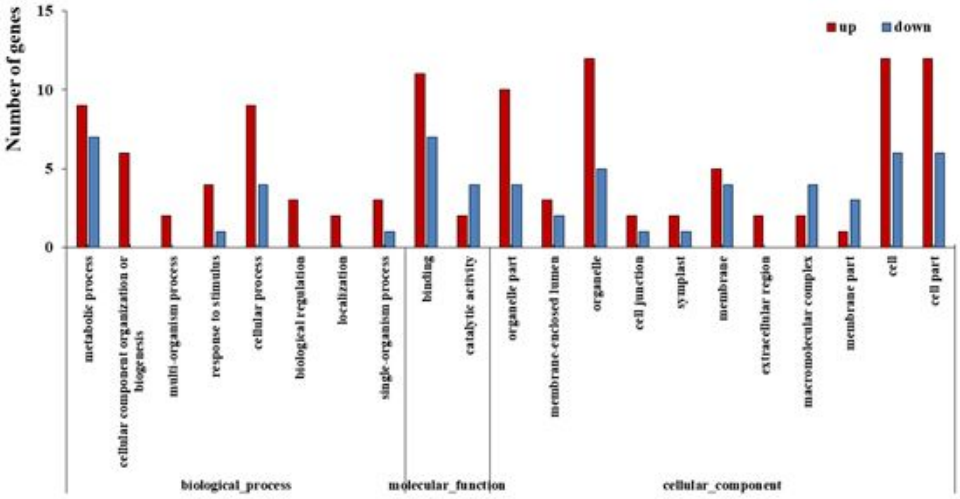

Figure 4

GO annotation of differentially expressed proteins between XM55 and YM158 under WL

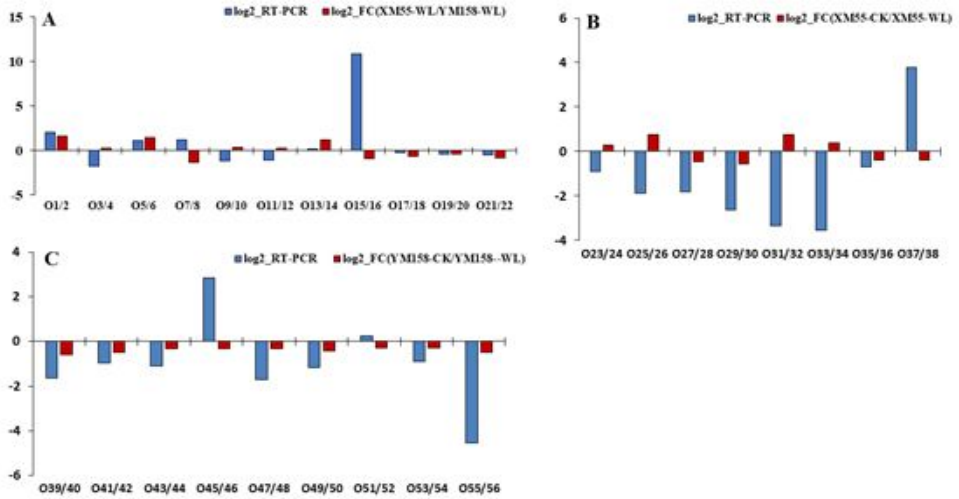

Figure 5

Correlation of differentially expressed protein at transcript and translation level. Differences in protein expression and qRT-PCR between XM55 and YM158 under waterlogging stress (A) Differences in protein expression measured by iTRAQ and quantitative real-time reverse transcription-PCR (qRT-PCR) in XM55 (B) and YM158 (C) under WL and CK. Log2-RT-PCR represents RNA expression level; Log2-FC represents the differences in protein expression level.

Supplementary Files

This is a list of supplementary files associated with this preprint. Click to download.

- supplement1.xlsx
- supplement2.jpg
- supplement3.docx
- supplement4.docx
- supplement5.docx
- supplement5.docx
- supplement7.xlsx
- supplement8.jpg